Bioorganic & Medicinal Chemistry 20 (2012) 877–885

Contents lists available at SciVerse ScienceDirect

Bioorganic & Medicinal Chemistry

journal homepage: www.elsevier.com/locate/bmc

Synthesis and biological evaluation of 4-[3-chloro-4-(3-fluorobenzyloxy) anilino]-6-(3-substituted-phenoxy)pyrimidines as dual EGFR/ErbB-2 kinase inhibitors

Siyuan Li [a], Chunying Guo [a], Hongli Zhao [a], Yun Tang [c], Minbo Lan [a,b,*]

[a] Shanghai Key Laboratory of Functional Materials Chemistry, Research Centre of Analysis and Test, East China University of Science and Technology, Shanghai 200237, PR China
[b] State Key Laboratory of Bioreactor Engineering, East China University of Science and Technology, Shanghai 200237, PR China
[c] Department of Pharmaceutical Science, School of Pharmacy, East China University of Science and Technology, Shanghai 200237, PR China

ARTICLE INFO

Article history:
Received 23 October 2011
Revised 25 November 2011
Accepted 25 November 2011
Available online 3 December 2011

Keywords:
Pyrimidine
EGFR
ErbB-2
Inhibitor
Docking

ABSTRACT

A series of 4-[3-chloro-4-(3-fluorobenzyloxy)anilino]-6-(3-substituted-phenoxy)pyrimidine derivatives were elaborately designed based on the skeleton of Lapatinib, and evaluated for their potential to inhibit epidermal growth factor receptor (EGFR) and ErbB-2 tyrosine kinase activities and antiproliferative activities against A431 and SKOV-3 cell lines. Among these synthesized pyrimidine derivatives, 4-[3-chloro-4-(3-fluorobenzyloxy)anilino]-6-(3-acrylamidophenoxy)pyrimidine (**6**), 4-[3-chloro-4-(3-fluorobenzyloxy)anilino]-6-(3-cyanoacetamidophenoxy)pyrimidine (**9**), 4-[3-chloro-4-(3-fluorobenzyloxy)anilino]-6-{3-[6-(4-amino)pyrimidinyl]amino) phenoxy}pyrimidine (**11**) and 4-[3-chloro-4-(3-fluorobenzyloxy)anilino]-6-(3-phenoxyacetamidophenoxy)pyrimidine (**14**) could significantly inhibit dual EGFR/ErbB-2 kinase activities (IC_{50} = 37/29 nM, 48/38 nM, 61/42 nM, 65/79 nM, respectively). And compounds **6** and **11** also showed the most potent antiproliferative activities in vitro, with the IC_{50} value of **6** being 3.25 μM for A431 and 0.89 μM for SKOV-3, as for **11**, 4.24 μM for A431 and 0.71 μM for SKOV-3, respectively. Docking study was also performed to determine the possible binding model.

1. Introduction

The human epidermal growth factor receptor (EGFR) is a transmembrane glycoprotein consisting of a single polypeptide chain of 1186 amino acids.[1,2] This receptor belongs to the ErbB/HER family of ligand-activated RTKs, which is catalytically active and under tight regulatory control.[3] EGF receptors play a key role in cell development, proliferation and differentiation within a variety of tissues.[4] Deregulation of their activity is extremely associated with tumorigenesis, such as lung cancer, breast cancer, ovarian cancer and colorectal cancer et al. Therefore EGFR is a key target for anti-tumor strategy.

In the past few years, a few kinds of compounds differing in structure, such as 4-anilinoquinazolines,[5,6] 4-anilinoquinoline-3-carbonitriles,[7] 1*H*-pyrazolo[3,4-*d*]pyrimidines,[8] pyrrolotriazines[9,10] and 4-amino-6-arylaminopyrimidines,[11,12] were reported as EGFR tyrosine kinase inhibitors. 4-Anilinoquinazoline, especially, was an excellent core to be modified as EGFR inhibitors, and some of these have been approved by FDA. Lapatinib, for example, is a potent dual EGFR/ErbB2 inhibitor approved for treatment of breast cancer (Fig. 1).[13]

It is known from the crystal structure of the Lapatinib–EGFR complex[14] and previous structure–activity relationship (SAR) of 4-anilinoquinazolines,[5,6,15–18] the binding mode is that Lapatinib places the aniline portion deep in the ATP binding site of the EGFR kinase, and this can affect kinase selectivity of ErbB family. An hydrogen bond is formed between N1 of the quinazoline and the main chain NH of Met 769, and another water-mediated one is formed between N3 and the side chain of Thr830.[14] Therefore, the 4-[3-chloro-4-(3-fluorobenzyloxy)anilino]pyrimidine is the most important portion between the interaction of Lapatinib and EGFR. Considering that we split the anilinoquinazoline into two pieces including a pyrimidine portion and a benzene ring, and

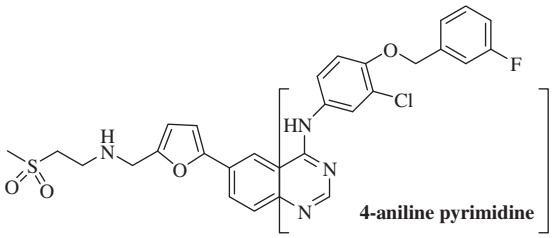

Figure 1. Dual EGFR/ErbB-2 inhibitors: Lapatinib.

* Corresponding author. Tel.: +86 21 64253574; fax: +86 21 64252947.
E-mail address: minbolan@ecust.edu.cn (M. Lan).

0968-0896/$ - see front matter © 2011 Elsevier Ltd. All rights reserved.
doi:10.1016/j.bmc.2011.11.056

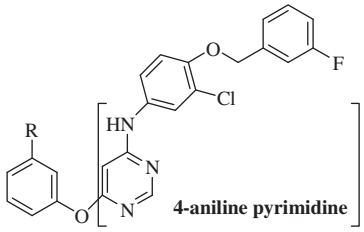

Figure 2. 4,6-Disubstituted pyrimidines.

insert an ether bond as a joint (Fig. 2). We believe these designed pyrimidine compounds might be potent to inhibit EGFR/ErbB-2 kinase activities as Lapatinib.

Herein, we disclose the synthesis of a series of 4,6-disubstituted pyrimidine compounds possessing 4-aniline pyrimidine portion together with their biological activities in vitro.

2. Chemistry

The synthetic route to 4-chloro-6-(3-nitrophenoxy)pyrimidine **2** began with a 4,6-dichloropyrimidine **1** and sodium *m*-nitrophenolate at room temperature in the presence of DMF (Scheme 1). Alternatively, *m*-nitrophenol was used for this reaction in the *n*-BuOH at reflux instead of sodium *m*-nitrophenolate, but the reaction of sodium *m*-nitrophenolate could give the highly quantitative product **2**. 4-[3-Chloro-4-(3-fluorobenzyloxy)anilino]-6-(3-nitrophenoxy)pyrimidine **3** was produced via a S_NAr reaction of **2** with 3-chloro-4-(3-fluorobenzyloxy)aniline. Selective reduction of the nitro group versus the aromatic halogen was accomplished by utilizing a system of iron powder and acetic acid to generate the desired intermediate product **4** with considerable yield.

The target molecules **5**–**19** were synthesized using intermediate product **4** by different methods (Scheme 2). Regarding molecules **6–7**, **9–10** and **13–19**, they were synthesized according to reacting with different acyl chlorides and same intermediate product **4** by method A or condensing **4** and carboxylic acid by method B. For examples, molecule **6** was prepared by acylation of **4** using acryloyl chloride with yield of 87%, and molecule **9** was obtained by

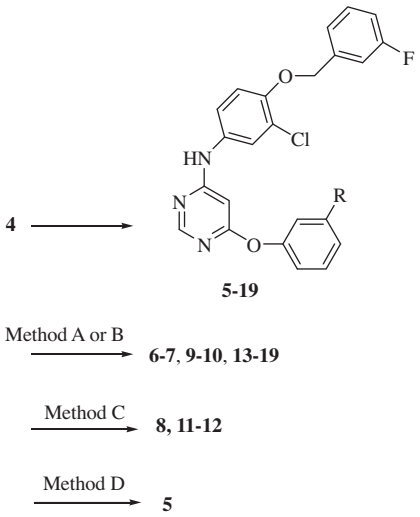

Scheme 2. Reagents and conditions: Method A: acyl chlorides, THF, rt, 80–95%. Method B: carboxylic acid, HOBt, EDC, THF, rt, 60–90%. Method C: halogenated compounds, *n*-BuOH, 110 °C, 52–90%. Method D: anhydride acetate, 80 °C, 95%.

condensing **4** with cyanoacetic acid using EDC and HOBt condensation system in THF. To synthesize the molecules **8**, **11** and **12**, corresponding halogenated compounds were used in the process of preparation by method C. Compound **12**, it was created via a nucleophilic substitution reaction using **4** and bromomethylbenzene as reactants in the solvent of *n*-BuOH. Intermediate product **4** was heated with anhydride acetate at 80 °C to yield the product **5**.

3. Results and discussion

3.1. Assay for in vitro activity

In pursuit of our goal to determine dual EGFR/ErbB-2 activities in the 4-[3-chloro-4-(3-fluorobenzyloxy)anilino]-6-(3-substituted-phenoxy)pyrimidine series, we evaluated the molecules **3–19** for EGFR/ErbB-2 inhibitory potency using homogeneous time-resolved

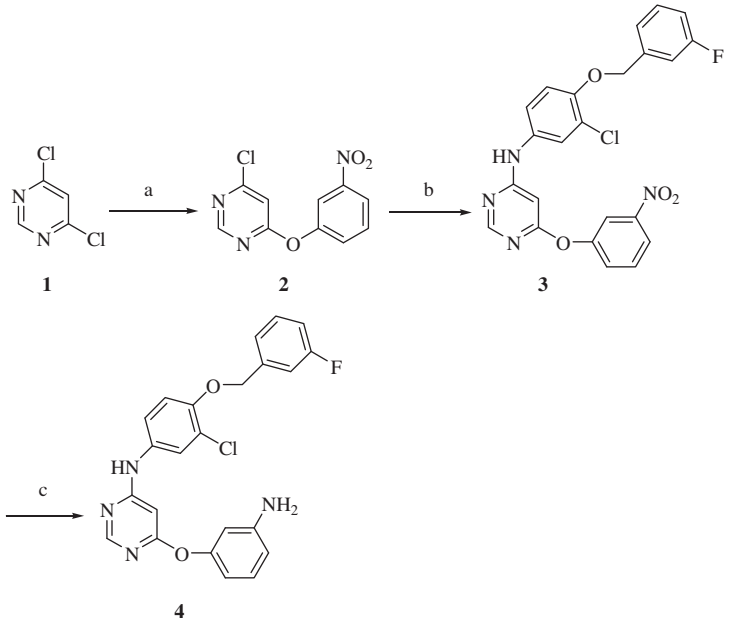

Scheme 1. Reagents and conditions: (a) sodium *m*-nitrophenolate, DMF, rt; (b) $ArNH_2$, *n*-BuOH, 110 °C; (c) Fe, CH_3COOH, ethanol, rf.

Table 1
In vitro evaluation of compound **3–19**

Compound	R	EGFR[a] (nM)	ErbB-2[a] (nM)	A431[b] (μM)	SKOV-3[b] (μM)
3	$-NO_2$	1204	2421	10.43	>30
4	$-NH_2$	473	559	8.92	12.21
5	$-NHCOCH_3$	108	135	12.02	3.95
6	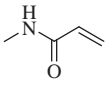	37	29	3.25	0.89
7	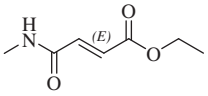	129	196	7.00	1.29
8	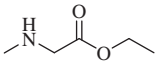	370	219	6.23	9.18
9	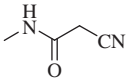	48	38	5.17	8.42
10	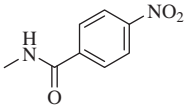	>10,000	>10,000	6.72	10.21
11	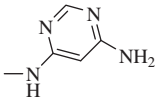	61	42	4.24	0.71
12	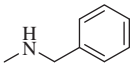	>10,000	>10,000	3.11	17.91
13	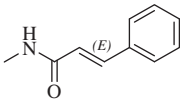	1671	3740	11.24	20.71
14	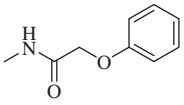	65	79	14.91	9.10
15	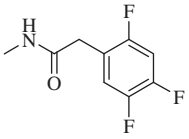	627	834	9.29	26.10
16	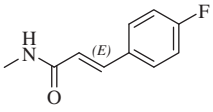	821	1293	18.12	>30
17	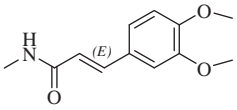	523	1234	>20	>30
18	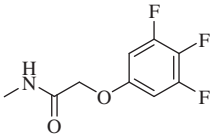	721	2138	13.25	>30
19	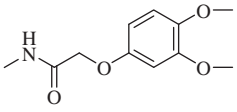	>10,000	>10,000	6.42	.02
Lapatinib		9.0	10.3	2.62	2.99

[a] The kinase inhibitory activities were determined using HTRF assay with compounds concentration 0.01–10,000 nM. The values are the average of at least two independent experiments performed in duplicate.

[b] The cell proliferation in A431 and SKOV-3 cells were determined by the MTT assay, after 72 h of incubation with compounds (0.05–30 μM). The values are the average of at least two independent experiments performed in duplicate.

fluorescence (HTRF) KinEASE-TK assay[19] from Cisbio according to manufacture's instruction. Lapatinib, with its high potency to EGFR (9.0 nM) and ErbB-2 (10.3 nM), was chosen as a standard compound in our kinase assay.

As summarized in Table 1, the various substituted groups on 3-phenoxy in the pyrimidine core, obviously, play an important role in kinase inhibitory activities. Amino group substituted on 3-phenoxy is better for kinase inhibitory activities than nitro group (IC_{50}: 473 vs 1204 nM for EGFR and 559 vs 2421 nM for ErbB-2), which means that electron donating groups is more potent than electron withdrawing groups on 3-phenoxy. 3-Phenoxy modified with kinds of side chains may improve potency, and although all of the synthesized compounds' kinase inhibitory activities are lower than Lapatinib, the compounds **6**, **9**, **11** and **14** hold the most potency for EGFR/ErbB-2. Among them compound **6**, gained by substitution with acrylamide, is the most potent one for EGFR (37 nM) and ErbB-2 (29 nM) than any other substituted type. Inhibitory activity of compound **9** (IC_{50}: 48 nM for EGFR; 38 nM for ErbB-2) is close to **6**, while compounds **5**, **7** and **8** are inferior to **6** with inhibitory activities at hundred nanomole order of magnitude. For the substituted types of compounds **3–9**, acrylamide and cyanoacetamide (**6** and **9**) are the most favorable groups with higher potency.

Compounds **11** and **14**, substituted with 4-aminopyrimidine or benzyloxy acetamide, are another series bearing a little bigger steric hindrance on 3-phenoxy with good inhibitory activities (IC_{50}: EGFR: 61 nM, ErbB-2: 42 nM for **11** and EGFR: 65 nM, ErbB-2: 79 nM for **14**). Other compounds have lower kinase inhibitory activities, even no activities among which **10**, **12** and **19** (IC_{50} >10,000 nM).

From Table 1, it is natural to come to the conclusion that small steric hindrance aliphatic chains are more helpful improving activities than bigger steric hindrance aromatic ring substituted chains. These aliphatic chains are probably more flexible for possessing the more and the better position selectivity when binding in the ATP binding domain of EGFR. Thus aliphatic chains substituted molecules such as **5–9** had the EGFR/ErbB-2 inhibitory activities more or less, while some of the compounds with aromatic ring substituted chains did not show any kinase inhibitory activities.

All of these molecules were also tested in cell proliferation assays by MTT method[20] using A431 and SKOV-3 cell lines which is overexpress EGFR and ErbB-2, respectively.[21] In cell assay, the IC_{50} values of Lapatinib were 2.62 and 2.99 μM for A431 and SKOV-3 cancer cell lines, respectively. Among compounds **6**, **9**, **11** and **14**, **9** and **14** showed minimal potency in antiproliferation assays in cancer cell lines even though it had reasonable levels of target potency at the enzyme level while compounds **6** and **11** showed approving potency contrasted to **9** and **14**. In our assay, treatment of A431 cells with compounds **6** and **11** resulted in decreased cell growth rate and their IC_{50} values were 3.25 and 4.24 μM which were closed to IC_{50} value of Lapatinib. Notably, compounds **6** and **11** inhibited SKOV-3 cell lines intensively with IC_{50} values being 0.89 and 0.71 μM, which resulted in 3.4- and 4.2-fold enhancement of cellular activities in contrasted to Lapatinib.

Interestingly, compound **12** had a favorable activity on A431 cell lines (IC_{50}=3.11 μM) and **5**, **7** were potent to SKOV-3 cell lines (IC_{50}=3.95 μM for **5**; 1.29 μM for **7**). Cell activities of these compounds were inconsistent with their kinase assay data possibly because **5**, **7** and **12** might inhibit other key proteins involved in the A431 and SKOV-3 cells proliferation, especially, for compound **12** which was ineffective to EGFR/ErbB-2 at all.

3.2. Docking study

To rationalize our design and our biological activity assay, docking study was carried out for docking the bioactive compounds **6**, **9**, **11** and **14** into EGFR using Glide 5.5.[22] Crystal structure of EGFR was downloaded from PDB database (PDB ID: 1XKK).[14]

Figure 3A demonstrates compound **6** was docking into ATP binding site of EGFR kinase. In the binding model, compound **6** was nicely bound to the ATP catalytic domain of the EGFR and formed two hydrogen bonds with the EGFR. One was formed between N1 of the **6** and main chain NH of Met793, and the distance was 2.431 Å while the angle value was 164.1°; another was formed between N3 and side chain OH of Thr854 through a water-mediated hydrogen bond. And an intermolecular hydrogen bond formed in the binding pose of **6** between NH of aniline and C═O of acrylamide group. The 3-chloro-4-(3-fluorobenzyloxy)aniline group was oriented deep in the back of the ATP binding site and made predominantly hydrophobic interactions with the protein. The pyrimidine ring was sandwiched from the top and bottom by the side chains of Ala743 and Leu844, respectively. And the phenoxy group of **6** was also at hydrophobic pocket and made slightly weak hydrophobic interactions with the residue of Leu718 and Leu844. The acrylamide group was located nearby the Arg841 and Asn842, hence electrostatic interactions formed. Thus this pose of **6** is much reasonable and **6** is the most potent in our synthesized compounds.

Compound **9** was also bound to EGFR commendably and the binding pose is similar to **6** (Fig. 3B). A hydrogen bond also formed between N1 of **9** and Met793, and the distance was 2.491 Å, the angle value 169.3°. N3 of **9** also interacted with a water molecule by a hydrogen bond. Cyanoacetamide chain of **9** oriented to a negative electrical area consisting of Val717, Leu718, Leu1001 and Met1002, though the distance to cyanoacetamide was relatively long (>3.7 Å), a very weak electrostatic repulsion remained between cyano group and these residues. Because of this position and orientation of cyanoacetamide in the pose, compound **9** shows a little weak kinase inhibitory activities in contrasted to **6**.

The binding model of compounds **11** and **14** was disclosed in Figure 3C and D, and the model was analogous to **6** and **9**. In the model of **11** and **14**, two similar hydrogen bonds were also formed same as models of compounds **6** and **9**. However, for **11,** a hydrogen bond emerged between NH_2 of **11** and C═O of Ser720 and the distance was 2.063 Å. The extra hydrogen bond was essential for **11** which was much more potent than other aromatic chains substituted compounds. Around the peripheral domain of the ATP binding site there was a negative electrical area consisting of residues of Asn842(C═O), Arg841(C═O) and Asp855(COO^-) which generated electrostatic repulsion effect to π-electron of amino pyrimidine ring resulting in pushing the pyrimidine ring leaning on the side of Ser720 and Gly721. Although the pose of **11** is much reasonable, the electrostatic repulsion effect is always exists to some extent while EGFR/ErbB-2 inhibitory activities of compound **11** is little lower than **6** and **9**. For compound **14**, though the aromatic ring chain is longer and more flexible than **11**, enough to make the benzene ring rotate to avoid the electrostatic repulsion and it is well complementary with van der waals surface of EGFR, the aromatic ring chain doesn't pick up any residue forming hydrogen bond which is more important for EGFR binding in these aromatic ring chain substituted compounds and the IC_{50} values of **14** is little higher than compound **11**. In addition, substitution with large negative electrical group in the aromatic ring such as -F results in decreasing the activities, because some negative electrical areas are distributed around the peripheral domain of active pocket, for instance an area comprising residues of Asn842(C═O), Arg841(C═O) and Asp855(COO^-) mentioned above, a second area consisting of residues of Leu718(C═O) and Val717(C═O), the third area consisting of residues of Ala1000(C═O), Leu1001(C═O) and Met1002(C═O, S) as well as the area consisting of residue of Asp800(COO^-), which repulse the negative electrical substituted groups that is harmful to kinase inhibitory effect.

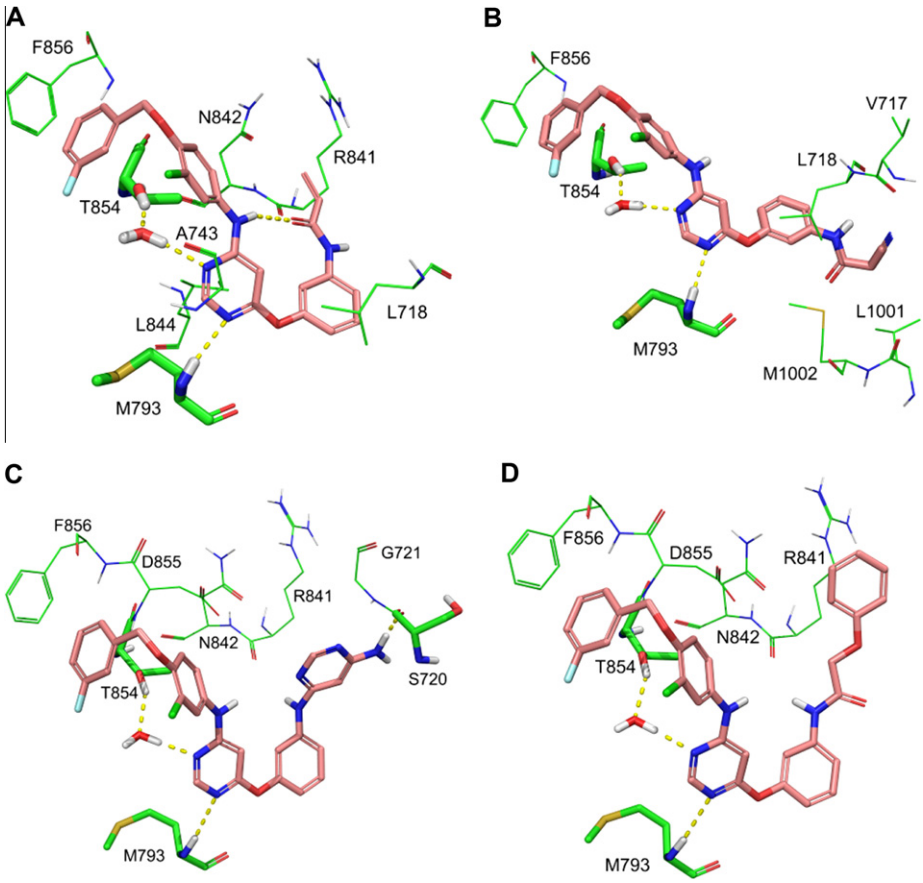

Figure 3. Binding models of compound **6**, **9**, **11** and **14** with EGFR corresponding to the left top sign A, B, C and D, respectively. The carbon in EGFR was colored in green, ligand carbons were colored in brown. Hydrogen bond was represented with yellow dashed line.

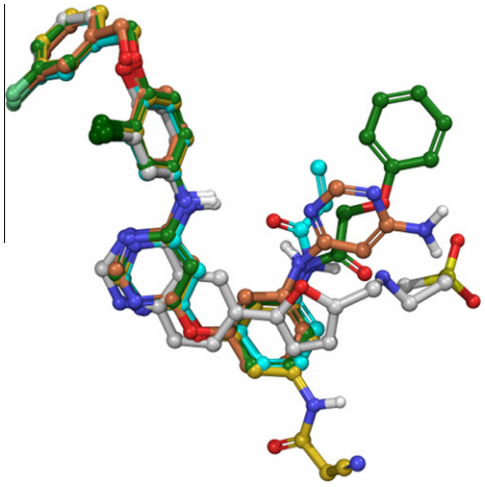

Figure 4. Overlay of compounds **6** (cyan), **9** (yellow), **11** (brown) and **14** (dark green) with Lapatinib (white).

The overlay of docking pose as shown in Figure 4 indicates the compounds **6**, **9**, **11** and **14** place the 4-[3-chloro-4-(3-fluorobenzyloxy)anilino]-6-(3-phenoxy) pyrimidine skeleton into a similar orientation as Lapatinib while some differences in substitution on 3-phenoxy. This suggests 4-[3-chloro-4-(3-fluorobenzyloxy)anilino] pyrimidine portion is the key skeleton for EGFR kinase inhibitory activity of this series and the various substitutions on 3-phenoxy result in different activities.

Our docking study shows that compounds **6**, **9**, **11** and **14** possess rational poses in binding with EGFR. Besides, these structural details gained from the binding models provide us useful information to elaborate the better potent inhibitors.

4. Conclusion

In this paper, a series of pyrimidine derivatives **3–19** based on the structure feature of Lapatinib has been synthesized and evaluated for their biological activities in vitro. Compounds **6**, **9**, **11** and **14** showed the most potent EGFR/ErbB-2 inhibition activities (IC_{50} = 37/29 nM, 48/38 nM, 61/42 nM, 65/79 nM, respectively). And the **6** and **11** displayed the excellent antiproliferative activities in vitro, with an IC_{50} value of 3.25 μM for A431 and 0.89 μM for SKOV-3 (**6**) while 4.24 μM for A431 and 0.71 μM for SKOV-3 (**11**). Docking study was performed to determine the possible binding model. From our model, it is indicated that the hydrogen bond interaction with residues Met793 and Thr854 of the protein in the ATP binding domain plays a key role in inhibition of EGFR/ErbB-2 activities. And the docking poses of compounds **6**, **9**, **11** and **14** were similar to Lapatinib, which proved our initial design. From these synthesized compounds, it is concluded that the **6** and **11**, as potential anticancer agent, showed the best dual EGFR/ErbB-2 and cancer cell proliferative inhibitory activities. This work might be helpful in further structure elaboration targeting more potent dual EGFR/ErbB-2 inhibitors.

5. Experimental

5.1. Chemistry

Melting points were determined in open capillary tubes on a SGW X-4 micro melting point apparatus and were uncorrected. Electron impact mass spectra were obtained on a Micromass GCT spectrometer. ^{1}H NMR spectra were measured on Brucker 400 MHz in δ scale. The spectra were obtained with solutions of $CDCl_3$ or DMSO-d_6 with TMS as internal standard, and the values of the chemical shifts (δ) were given in ppm, coupling constants (J) given in Hz. Elemental analyses were carried out at VARIO ELIII apparatus and were within ±0.4%.

5.1.1. 4-Chloro-6-(3-nitrophenoxy)pyrimidine (2)

A mixture of 4,6-dichloropyrimidine (**1**) (5.00 g, 33.55 mmol) and sodium *m*-nitrophenolate (5.41 g, 33.55 mmol) in DMF (20 mL) was stirred at ambient temperature under N_2 protection for 30 min. The mixture was diluted with 80 mL EtOAc and washed with brine (3 × 50 mL). The organic layer was dried over anhydrous $MgSO_4$, the solvent was removed, and the residue was washed with hexane (30 mL) to give **2** as a canary yellow solid (8.02 g, 31.87 mmol, 95% yield). Mp: 45–47 °C; ^{1}H NMR (400 MHz, $CDCl_3$) δ 7.09(s, 1H), δ 7.55(dd, 1H, J = 4.0 Hz, 8.0 Hz), δ 7.66(t, 1H, J = 8.0 Hz), δ 8.06(t, 1H, J = 2.4 Hz), δ 8.18(dd, 1H, J = 4 Hz, 8.0 Hz), δ 8.57(s, 1H); MS (EI) m/e 251.0 (M^+); Anal. Calcd for $C_{10}H_6ClN_3O_3$: C, 47.73; H, 2.40; N, 16.70. Found: C, 47.94; H, 2.56; N, 17.01.

5.1.2. 4-[3-Chloro-4-(3-fluorobenzyloxy)anilino]-6-(3-nitro phenoxy)pyrimidine (3)

A mixture of 3-chloro-4-(3-fluorobenzyloxy)aniline (5.00 g, 19.86 mmol) and compound **2** (4.17 g, 16.55 mmol) with two drops concd HCl in *n*-BuOH (30 mL) was heated at 110 °C and kept stirring for 3 h. As the mixture cooled, the formed yellow solid was filtered through washing with *n*-BuOH followed by saturated $NaHCO_3$ aqueous solution. After being dried overnight at vacuum drying oven at 40 °C, the solid was purified by column chromatography on silica gel eluted with EtOAc/petroleum ether (1:2) to give **3** as a yellowish green solid (6.18 g, 13.24 mmol, 80% yield). Mp: 138–140 °C; ^{1}H NMR (400 MHz, DMSO-d_6) δ 5.21(s, 2H), δ 6.30(s, 1H), δ 7.15–7.22(m, 2H), δ 7.28–7.32(m, 2H), δ 7.44–7.49(m, 2H), δ 7.70–7.77(m, 2H), δ 7.88(d, 1H, J = 2.4 Hz), δ 8.07(t, 1H, J = 2.0 Hz, 2.4 Hz), δ 8.14(dt, 1H, J = 2.0 Hz, 8.0 Hz), δ 8.37(s, 1H), δ 9.93(s, 1H); MS (EI) m/e 466.1 (M^+); Anal. Calcd for $C_{23}H_{16}ClFN_4O_4$: C, 59.17; H, 3.45; N, 12.00. Found: C, 59.07; H, 3.32; N, 11.82.

5.1.3. 4-[3-Chloro-4-(3-fluorobenzyloxy)anilino]-6-(3-amino phenoxy)pyrimidine (4)

A mixture of **3** (5.00 g, 10.71 mmol), iron powder (5.98 g, 107.1 mmol) and AcOH (7.50 g, 125.0 mmol) in ethanol (200 mL) was heated at reflux and kept intensively stirring for 2 h, and then another iron powder (5.98 g, 107.1 mmol) was added and kept stirring for another 2 h. As the mixture cooled, the mixture was filtered and washed with ethanol (50 mL), filtrate collected then evaporated under reduced pressure. The residue was diluted with saturated $NaHCO_3$ aqueous solution to generate brown solid. The solid was decolorized with activated carbon, and a crude product obtained. Further purification was carried out by recrystallization from CH_2Cl_2/THF to give **4** as a white solid (3.65 g, 8.35 mmol, 78% yield). Mp: 191–193 °C; ^{1}H NMR (400 MHz, DMSO-d_6) δ 5.20(s, 2H), δ 5.34(s, 2H), δ 5.97(s, 1H), δ 6.29(dd, 1H, J = 1.6 Hz, 8.0 Hz), δ 6.34(t, 1H, J = 2 Hz), δ 6.48(dd, 1H, J = 1.2 Hz, 8.0 Hz), δ 7.08(t, 1H, J = 8.0 Hz), δ 7.15–7.20(m, 2H), δ 7.28–7.32(m, 2H), δ 7.39(dd, 1H, J = 2.4 Hz, 8.0 Hz), δ 7.43–7.49(m, 1H), δ 7.86(d, 1H, J = 2.4 Hz), δ 8.36(s, 1H), δ 8.52(s, 1H); MS (EI) m/e 436.1 (M^+); Anal. Calcd for $C_{23}H_{18}ClFN_4O_2$: C, 63.23; H, 4.15; N, 12.82. Found: C, 63.44; H, 4.32; N, 12.60.

5.1.4. 4-[3-Chloro-4-(3-fluorobenzyloxy)anilino]-6-(3-acetam idophenoxy)pyrimidine (5)

Method D. A mixture of **4** (200 mg, 0.46 mmol) and acetic anhydride (6 mL) was heated at 80 °C for 1 h. The acetic anhydride was evaporated and the residue was dissolved in EtOAc (50 mL) and then washed with saturated $NaHCO_3$ aqueous solution (3 × 20 mL). The organic layer was dried over anhydrous $MgSO_4$, and the solvent was removed, purified by column chromatography on silica gel eluted with EtOAc/petroleum ether (1:2) to give **5** as a white solid (207 mg, 0.43 mmol, 95% yield). Mp: 165–167 °C; ^{1}H NMR (400 MHz, DMSO-d_6) δ 2.06(s, 3H), δ 5.20(s, 2H), δ 6.03(s, 1H), δ 6.87(dt, 1H, J = 2.0 Hz, 8.0 Hz), δ 7.17(s, 1H), δ 7.20(s, 1H), δ 7.28–7.32(m, 2H), δ 7.37–7.43(m, 3H), δ 7.45–7.49(m, 1H), δ 7.52(s, 1H), δ 7.86(d, 1H, J = 2.4 Hz), δ 8.36(s, 1H), δ 9.57(s, 1H), δ 10.11(s, 1H); MS (EI) m/e 478.1 (M^+); Anal. Calcd for $C_{25}H_{20}ClFN_4O_3$: C, 62.70; H, 4.21; N, 11.70. Found: C, 62.67; H, 3.94; N, 11.35.

5.1.5. 4-[3-Chloro-4-(3-fluorobenzyloxy)anilino]-6-(3-acrylam idophenoxy)pyrimidine (6)

Method A. A solution of THF (5 mL) containing acryloyl chloride (45 mg, 0.50 mmol) was added to another solution of **4** (200 mg, 0.46 mmol) in anhydrous THF (10 mL) at 0 °C dropwise under N_2 atmosphere and then the mixture was stirred at room temperature for 30 min. After THF was removed under reduced pressure, the residue was purified by column chromatography on silica gel eluted with EtOAc/petroleum ether (1:1) to give **6** as a white solid (196 mg, 0.40 mmol, 87% yield). Mp: 180–182 °C; ^{1}H NMR (400 MHz, DMSO-d_6) δ 5.20(s, 2H), δ 5.79(dd, 1H, J = 2.0 Hz, 10.0 Hz), δ 6.06(s, 1H), δ 6.27(dd, 1H, J = 2.0 Hz, 16.0 Hz), δ 6.43(q, 1H, J = 2.0 Hz), δ 6.92(dd, 1H, J = 1.6 Hz, 8.0 Hz), δ 7.19(d, 2H, J = 8.0 Hz), δ 7.28–7.32(m, 2H), δ 7.38–7.52(m, 4H), δ 7.62(s, 1H), δ 7.86(d, 1H, J = 2.4 Hz), δ 8.37(s, 1H), δ 8.57(s, 1H), δ 10.32(s, 1H); MS (EI) m/e 490.1 (M^+); Anal. Calcd for $C_{26}H_{20}ClFN_4O_3$: C, 63.61; H, 4.11; N, 11.41. Found: C, 63.82; H, 4.15; N, 11.10.

5.1.6. 4-[3-Chloro-4-(3-fluorobenzyloxy)anilino]-6-(3-fumari camidophenoxy)pyrimidine (7)

Compound **7** was prepared from **4** (200 mg, 0.46 mmol) and fumaric chloride (81 mg, 0.50 mmol) in THF (15 mL) by the procedure described for **6** to give **7** as a white solid (202 mg, 0.36 mmol, 78% yield). Mp: 145–146 °C; ^{1}H NMR (400 MHz, DMSO-d_6) δ 1.27(t, 3H, J = 7.2 Hz), δ 4.22(q, 2H, J = 7.2 Hz), δ 5.21(s, 2H), δ 6.07(s, 1H), δ 6.71(d, 1H, J = 16.0 Hz), δ 6.96(dd, 1H, J = 1.2 Hz, 8.0 Hz), δ 7.15–7.22(m, 3H), δ 7.28–7.32(m, 2H), δ 7.38–7.42(m, 1H), δ 7.44–7.51(m, 3H), δ 7.63(t, 1H, J = 2.0 Hz), δ 7.86(d, 1H, J = 2.8 Hz), δ 8.37(s, 1H), δ 9.58(s, 1H), δ 10.73(s, 1H); MS (EI) m/e 562.2 (M^+); Anal. Calcd for $C_{29}H_{24}ClFN_4O_5$: C, 61.87; H, 4.30; N, 9.95. Found: C, 61.67; H, 4.09; N, 9.68.

5.1.7. 4-[3-Chloro-4-(3-fluorobenzyloxy)anilino]-6-[3-(2-ethoxycarbonylethylamino) phenoxy]pyrimidine (8)

Method C. A mixture of **4** (200 mg, 0.46 mmol) and ethyl bromoacetate (92 mg, 0.55 mmol) in pyridine (0.5 mL), in which, dioxane (7 mL) was added, was heated at 100 °C for 3 h. After removal of dioxane under reduced pressure, the residue was diluted with EtOAc (40 mL) then washed with saturated $NaHCO_3$ aqueous solution (3 × 15 mL). The organic layer dried over anhydrous $MgSO_4$, and the solvent was removed, purified by column chromatography on silica gel eluted with EtOAc/petroleum ether (3:5) to give **8** as a light yellow solid (125 mg, 0.24 mmol, 52% yield). Mp: 58–59 °C;

^{1}H NMR (400 MHz, DMSO-d_6) δ 1.22(t, 3H, J = 3.2 Hz), δ 3.80(s, 2H), δ 4.17(q, 2H, J = 7.2 Hz), δ 5.07(s, 2H), δ 5.95(s, 1H), δ 6.27(t, 1H, J = 2.4 Hz), δ 6.39–6.43(m, 2H), δ 6.86(d, 1H, J = 8.8 Hz), δ 6.93–6.98(m, 2H), δ 7.06(dd, 1H, J = 2.8 Hz, 8.4 Hz), δ 7.10–7.16(m, 3H), δ 7.19(s, 1H), δ 7.26–7.30(m, 1H), δ 7.33(d, 1H, J = 2.8 Hz), δ 8.28(s, 1H); MS (EI) m/e 522.2 (M^+); Anal. Calcd for $C_{27}H_{24}ClFN_4O_4$: C, 62.01; H, 4.63; N, 10.71. Found: C, 62.23; H, 4.75; N, 10.55.

5.1.8. 4-[3-Chloro-4-(3-fluorobenzyloxy)anilino]-6-(3-cyanoacetamidophenoxy)pyrimidine (9)

Method B. A mixture of **4** (200 mg, 0.46 mmol) and cyanoacetic acid (78 mg, 0.92 mmol) in THF (15 mL) in ice bath added with EDC (176 mg, 0.92 mmol) and HOBt (124 mg, 0.92 mmol) was stirred for 30 min. Having removed the ice bath, the mixture was stirred at room temperature overnight. After removing the solvent, the residue was dissolved in EtOAc (35 mL) washed with saturated $NaHCO_3$ aqueous solution (3 × 15 mL). The organic layer dried over anhydrous $MgSO_4$, and the solvent was removed, purified by column chromatography on silica gel eluted with EtOAc/petroleum ether (1:1) to give **9** as a white solid (155 mg, 0.31 mmol, 67% yield). Mp: 167–169 °C; ^{1}H NMR (400 MHz, DMSO-d_6) δ 3.92(s, 2H), δ 5.20(s, 2H), δ 6.06(s, 1H), δ 6.93(dt, 1H, J = 2.0 Hz, 7.2 Hz), δ 7.15–7.20(m, 2H), δ 7.27–7.32(m, 2H), δ 7.38–7.49(m, 5H), δ 7.85(d, 1H, J = 2.4 Hz), δ 8.35(s, 1H), δ 9.57(s, 1H), δ 10.46(s, 1H); MS (EI) m/e 503.1 (M^+); Anal. Calcd for $C_{26}H_{19}ClFN_5O_3$: C, 61.97; H, 3.80; N, 13.90. Found: C, 62.02; H, 3.73; N, 13.69.

5.1.9. 4-[3-Chloro-4-(3-fluorobenzyloxy)anilino]-6-(3-*p*-nitrobenzamidophenoxy)pyrimidine (10)

Compound **10** was prepared from **4** (200 mg, 0.46 mmol) and *p*-nitrobenzoyl chloride (93 mg, 0.50 mmol) in THF (15 mL) by the procedure described for **6** to give **10** as a yellow solid (186 mg, 0.32 mmol, 69% yield). Mp: 189–191 °C; ^{1}H NMR (400 MHz, DMSO-d_6) δ 5.32(s, 2H), δ 6.09(s, 1H), δ 7.00(dd, 1H, J = 1.6 Hz, 7.4 Hz), δ 7.15–7.20(m, 2H), δ 7.28–7.32(m, 2H), δ 7.40(dd, 1H, J = 2.4 Hz, 8.0 Hz), δ 7.43–7.50(m, 2H), δ 7.68–7.70(m, 2H), δ 7.86(d, 1H, J = 2.4 Hz), δ 8.18(s, 1H), δ 8.20(s, 1H), δ 8.38–8.40(m, 3H), δ 8.58(s, 1H), δ 10.71(s, 1H); MS (EI) m/e 585.1 (M^+); Anal. Calcd for $C_{30}H_{21}ClFN_5O_5$: C, 61.49; H, 3.61; N, 11.95. Found: C, 61.58; H, 3.28; N, 11.91.

5.1.10. 4-[3-Chloro-4-(3-fluorobenzyloxy)anilino]-6-{3-[6-(4-amino)pyrimidinyl] amino)phenoxy}pyrimidine (11)

Compound **11** was prepared from **4** (200 mg, 0.46 mmol), 4-amino-6-chloropyrimidine (71 mg, 0.55 mmol) and a drop of concd HCl in *n*-BuOH (10 mL) by the procedure described for **8** to give **11** as a white solid (219 mg, 0.41 mmol, 90% yield). Mp: 180–182 °C; ^{1}H NMR (400 MHz, DMSO-d_6) δ 5.20(s, 2H), δ 5.81(s, 1H), δ 6.02(s, 1H), δ 6.42(s, 2H), δ 6.73(dd, 1H, J = 1.6 Hz, 8.0 Hz), δ 7.15–7.20(m, 2H), δ 7.28–7.49(m, 6H), δ 7.55(s, 1H), δ 7.86(d, 1H, J = 2.4 Hz), δ 8.06(s, 1H), δ 8.37(s, 1H), δ 9.11(s, 1H), δ 9.55(s, 1H); MS (EI) m/e 529.2 (M^+); Anal. Calcd for $C_{27}H_{21}ClFN_7O_2$: C, 61.19; H, 3.99; N, 18.50. Found: C, 61.05; H, 3.77; N, 18.15.

5.1.11. 4-[3-Chloro-4-(3-fluorobenzyloxy)anilino]-6-(3-phenylethylaminophenoxy)pyrimidine (12)

Compound **12** was prepared from **4** (200 mg, 0.46 mmol) and benzyl bromide (94 mg, 0.55 mmol) in pyridine (0.5 mL) adding dioxane (8 mL) by the procedure described for **8** to give **12** as a light yellow solid (200 mg, 0.38 mmol, 83% yield). Mp: 60–62 °C; ^{1}H NMR (400 MHz, DMSO-d_6) δ 4.27(d, 2H, J = 6.0 Hz), δ 5.19(s, 2H), δ 5.95(s, 1H), δ 6.32(dd, 1H, J = 1.6 Hz, 8.0 Hz), δ 6.37(t, 1H, J = 2.0 Hz), δ 6.50–6.52(m, 2H), δ 7.10–7.41(m, 11H), δ 7.45(q, 1H, J = 8.0 Hz), δ 7.86(d, 1H, J = 2.8 Hz), δ 8.35(s, 1H), δ 9.51(s, 1H); MS (EI) m/e 526.2 (M^+); Anal. Calcd for $C_{30}H_{24}ClFN_4O_2$: C, 68.37; H, 4.59; N, 10.63. Found: C, 68.37; H, 4.85; N, 10.60.

5.1.12. 4-[3-Chloro-4-(3-fluorobenzyloxy)anilino]-6-(3-cinnamamidophenoxy)pyrimidine (13)

Compound **13** was prepared from **4** (200 mg, 0.46 mmol) and cinnamoyl chloride (92 mg, 0.55 mmol) in THF (15 mL) by the procedure described for **6** to give **13** as a white solid (224 mg, 0.40 mmol, 86% yield). Mp: 178–181 °C; ^{1}H NMR (400 MHz, DMSO-d_6) δ 5.20(s, 2H), δ 6.07(s, 1H), δ 6.83(d, 1H, J = 15.6 Hz), δ 6.92(dd, 1H, J = 1.6 Hz, 8.0 Hz), δ 7.15–7.20(m, 2H), δ 7.27–7.31(m, 2H), δ 7.38–7.48(m, 6H), δ 7.52–7.54(m, 1H), δ 7.59–7.62(m, 2H), δ 7.64–7.67(m, 2H), δ 7.86(d, 1H, J = 2.4 Hz), δ 8.38(s, 1H), δ 9.57(s, 1H), δ 10.39(s, 1H); MS (EI) m/e 566.2 (M^+); Anal. Calcd for $C_{32}H_{24}ClFN_4O_3$: C, 67.78; H, 4.27; N, 9.88. Found: C, 68.02; H, 4.10; N, 9.63.

5.1.13. 4-[3-Chloro-4-(3-fluorobenzyloxy)anilino]-6-(3-phenoxyacetamidophenoxy)pyrimidine (14)

Compound **14** was prepared from **4** (200 mg, 0.46 mmol) and phenoxyacetic acid (140 mg, 0.92 mmol) in THF (15 mL) adding EDC (176 mg, 0.92 mmol) and HOBt (124 mg, 0.92 mmol) by the procedure described for **9** to give **14** as a white solid (163 mg, 0.29 mmol, 62% yield). Mp: 145–147 °C; ^{1}H NMR (400 MHz, DMSO-d_6) δ 4.71(s, 2H), δ 5.20(s, 2H), δ 6.05(s, 1H), δ 6.93(dd, 1H, J = 1.2 Hz, 8.0 Hz), δ 6.96–7.01(m, 3H), δ 7.15–7.20(m, 2H), δ 7.28–7.34(m, 4H), δ 7.38–7.48(m, 3H), δ 7.53–7.57(m, 2H), δ 7.85(d, 1H, J = 2.8 Hz), δ 8.36(s, 1H), δ 9.56(s, 1H), δ 10.24(s, 1H); MS (EI) m/e 570.2 (M^+); Anal. Calcd for $C_{31}H_{24}ClFN_4O_4$: C, 65.21; H, 4.24; N, 9.81. Found: C, 65.28; H, 4.01; N, 9.57.

5.1.14. 4-[3-Chloro-4-(3-fluorobenzyloxy)anilino]-6-[3-(2,4,5-trifluorophenylacetamido)phenoxy]pyrimidine (15)

Compound **15** was prepared from **4** (200 mg, 0.46 mmol) and 2,4,5-trifluorophenylacetic acid (175 mg, 0.92 mmol) in THF (15 mL) adding EDC (176 mg, 0.92 mmol) and HOBt (124 mg, 0.92 mmol) by the procedure described for **9** to give **15** as a white solid (210 mg, 0.35 mmol, 75% yield). Mp: 173–175 °C; ^{1}H NMR (400 MHz, DMSO-d_6) δ 3.75(s, 2H), δ 5.20(s, 2H), δ 6.04(s, 1H), δ 6.89(dt, 1H, J = 2.0 Hz, 7.2 Hz), δ 7.15–7.19(m, 2H), δ 7.27–7.32(m, 2H), δ 7.37–7.57(m, 7H), δ 7.84(d, 1H, J = 2.4 Hz), δ 8.35(s, 1H), δ 9.55(s, 1H), δ 10.39(s, 1H); MS (EI) m/e 608.1 (M^+); Anal. Calcd for $C_{31}H_{21}ClF_4N_4O_3$: C, 61.14; H, 3.48; N, 9.20. Found: C, 61.41; H, 3.30; N, 9.03.

5.1.15. 4-[3-Chloro-4-(3-fluorobenzyloxy)anilino]-6-(3-*p*-fluorocinnamamidophenoxy)pyrimidine (16)

Compound **16** was prepared from **4** (200 mg, 0.46 mmol) and 4-fluorocinnamic acid (153 mg, 0.92 mmol) in THF (15 mL) adding EDC (176 mg, 0.92 mmol) and HOBt (124 mg, 0.92 mmol) by the procedure described for **9** to give **16** as a white solid (175 mg, 0.30 mmol, 65% yield). Mp: 205–207 °C; ^{1}H NMR (400 MHz, DMSO-d_6) δ 5.20(s, 2H), δ 6.07(s, 1H), δ 6.77(d, 1H, J = 16 Hz), δ 6.92(dd, 1H, J = 2.4 Hz, 8.0 Hz), δ 7.15–7.20(m, 2H), δ 7.27–7.31(m, 4H), δ 7.38–7.48(m, 3H), δ 7.53(d, 1H, J = 8.4 Hz), δ 7.60(d, 1H, J = 15.6 Hz), δ 7.66(s, 1H), δ 7.68–7.72(m, 2H), δ 7.86(d, 1H, J = 2.8 Hz), δ 8.38(s, 1H), δ 9.57(s, 1H), δ 10.38(s, 1H); MS (EI) m/e 584.2 (M^+); Anal. Calcd for $C_{32}H_{23}ClF_2N_4O_3$: C, 65.70; H, 3.96; N, 9.58. Found: C, 65.96; H, 3.83; N, 9.24.

5.1.16. 4-[3-Chloro-4-(3-fluorobenzyloxy)anilino]-6-[3-(3,4-dimethoxycinnamamido)phenoxy]pyrimidine (17)

Compound **17** was prepared from **4** (200 mg, 0.46 mmol) and 3,4-dimethoxycinnamoyl chloride (125 mg, 0.55 mmol) in THF (15 mL) by the procedure described for **6** to give **17** as a white solid (239 mg, 0.38 mmol, 83% yield). Mp: 188–191 °C; ^{1}H NMR (400 MHz, DMSO-d_6) δ 3.80(s, 3H), δ 3.82(s, 3H), δ 5.20(s, 2H), δ 6.06(s, 1H), δ 6.69(d, 1H, J = 15.6 Hz), δ 6.90(dd, 1H, J = 1.6 Hz, 8.0 Hz), δ 7.02(d, 1H, J = 8.4 Hz), δ 7.14–7.22(m, 4H), δ 7.27–

7.31(m, 2H), δ 7.38–7.47(m, 3H), δ 7.48–7.56(m, 2H), δ 7.66(s, 1H), δ 7.85(d, 1H, *J* = 2.8 Hz), δ 8.37(s, 1H), δ 9.57(s, 1H), δ 10.30(s, 1H); MS (EI) *m*/*e* 626.2 (M^+); Anal. Calcd for $C_{34}H_{28}ClFN_4O_5$: C, 65.12; H, 4.50; N, 8.93. Found: C, 65.26; H, 4.26; N, 8.67.

5.1.17. 4-[3-Chloro-4-(3-fluorobenzyloxy)anilino]-6-[3-(3,4,5-trifluorophenoxyacetamido)phenoxy]pyrimidine (18)

Compound **18** was prepared from **4** (200 mg, 0.46 mmol) and 3,4,5-trifluorophenoxyacetic chloride (124 mg, 0.55 mmol) in THF (15 mL) by the procedure described for **6** to give **18** as a white solid (219 mg, 0.35 mmol, 76% yield). Mp: 153–155 °C; ^1H NMR (400 MHz, DMSO-d_6) δ 4.77(s, 2H), δ 5.21(s, 2H), δ 6.06(s, 1H), δ 6.94(dd, 1H, *J* = 1.6 Hz, 8.4 Hz), δ 7.03–7.10(m, 2H), δ 7.15–7.20(m, 2H), δ 7.28–7.32(m, 2H), δ 7.38–7.54(m, 5H), δ 7.85(d, 1H, *J* = 2.4 Hz), δ 8.36(s, 1H), δ 9.57(s, 1H), δ 10.23(s, 1H); MS (EI) *m*/*e* 624.1 (M^+); Anal. Calcd for $C_{31}H_{21}ClF_4N_4O_4$: C, 59.58; H, 3.39; N, 8.96. Found: C, 59.82; H, 3.63; N, 8.63.

5.1.18. 4-[3-Chloro-4-(3-fluorobenzyloxy)anilino]-6-[3-(3,4-dimethoxyphenoxyacetamido)phenoxy]pyrimidine (19)

Compound **19** was prepared from **4** (200 mg, 0.46 mmol) and 3,4-dimethoxyphenoxyacetic chloride (127 mg, 0.55 mmol) in THF (15 mL) by the procedure described for **6** to give **19** as a white solid (255 mg, 0.41 mmol, 88% yield). Mp: 130–132 °C; ^1H NMR (400 MHz, DMSO-d_6) δ 3.69(s, 3H), δ 3.75(s, 3H), δ 4.64(s, 2H), δ 5.20(s, 2H), δ 6.05(s, 1H), δ 6.49(dd, 1H, *J* = 2.8 Hz, 8.8 Hz), δ 6.72(d, 1H, *J* = 2.8 Hz), δ 6.87(d, 1H, *J* = 8.8 Hz), δ 6.92–6.94(m, 1H), δ 7.15–7.20(m, 2H), δ 7.28–7.32(m, 2H), δ 7.38–7.49(m, 3H), δ 7.55–7.57(m, 2H), δ 7.85(d, 1H, *J* = 2.4 Hz), δ 8.36(s, 1H), δ 9.57(s, 1H), δ 10.18(s, 1H); MS (EI) *m*/*e* 630.2 (M^+); Anal. Calcd for $C_{33}H_{28}ClFN_4O_6$: C, 62.81; H, 4.47; N, 8.88. Found: C, 62.50; H, 4.27; N, 8.63.

5.2. Kinase assay

The kinase inhibition assay and IC_{50} determinations for wild type EGFR/ErbB-2 were measured with the homogeneous time-resolved fluorescence (HTRF) KinEASE-TK assay from Cisbio according to the manufacturer's instructions. Wild type EGFR(669–1210) and ErbB-2(676–1255) was purchased from Carna Biosciences and 0.09 and 0.11 ng/μL kinase were used for test, respectively. ATP concentration was set at its K_m values (23 and 39 μM for EGFR and ErbB-2), and 180 nM substrate were used for both EGFR and ErbB-2. Kinase, substrate peptide and inhibitors were added in 384 well plates, and then reaction was started by addition of ATP. After completion of the reaction, an antiphosphotyrosine antibody labeled with europium cryptate and streptavidin labeled with the fluorophore XL665 were added. The FRET between europium cryptate and XL665 was measured to quantify the phosphorylation of the substrate peptide. A Tecan i-control infinite 500 was used to measure the fluorescence of the samples at 620 nM (Eu-labeled antibody) and 665 nM (XL665 labeled streptavidin) 500 μs after excition at 320 nM. The quotient of both intensities for reactions made with ten different inhibitor concentrations (0.01–10,000 nM, including no inhibitor) was plotted against inhibitor concentrations to determine IC_{50} values. Each reaction was performed in duplicate, and at least two independent determinations of each IC_{50} were made.

5.3. Cell growth assay

Human epidermoid carcinoma cells (A431) and human ovarian carcinoma cells (SKOV-3) were routinely grown at 37 °C in a humidified incubator with 5% CO_2 in DMEM medium supplemented with 10% fetal bovine serum (FBS), 2 mM glutamine, 50 U/mL penicillin and 50 μg/mL streptomycin. To determine the cell proliferation, the A431 and SKOV-3 cells were seeded in 96-well plates at 1×10^4 cells/well. All experiments were performed after 24 h of incubation at 37 °C in 5% CO_2.

The cell proliferation was evaluated with the MTT(3-(4,5-dimethyl-2-thiazolyl)-2,5-diphenyl-2*H*-tetrazolium bromide) assay, as described by Mosmann.[20] Briefly, A431 and SKOV-3 cells were treated with compounds (0.05–30 μM) for 72 h at 37 °C in 5% CO_2. After that, the cells were washed with phosphate buffered saline (PBS) and then incubated with MTT (5 mg/mL) in DMEM medium for 4 h. After removal of MTT and further washing, the formazan crystals were dissolved with DMSO. The amount of formazan was measured (492 nm, 630 nm) with a spectrophotometer.

The cell viability was expressed in percentage of control cells and calculated by the formula $F_t/F_{nt} \times 100$, where F_t = absorbance of treated cells and F_{nt} = absorbance of untreated cells. At least two independent dose–response curves were done and the concentration of compound resulting in 50% inhibition of cell proliferation (IC_{50}) was calculated.

5.4. Docking study

Molecular docking of compounds **6**, **9**, **11** and **14** was performed using Glide 5.5.[22] Crystal structure of EGFR was downloaded from the Protein Data Bank (PDB ID: 1XKK). In precise, the protein structure was prepared with the Protein Preparation Wizard.[22] With respect to the ligands, LigPrep[23] was employed to prepare all of them. And then Glide 5.5 was used to dock the four compounds into the binding pocket. All graphical pictures were made using the Pymol program.

Acknowledgments

This work was supported by the Ministry of Science and Technology of the People's Republic of China (Contract No. 2010DFA44300), National Natural Science Foundation of China (NSFC, Contract No. 21074033) and the Science and Technology Commission of Shanghai Municipality (STCSM, No. 10dz2220500). We also thank Wen Xiao from School of Pharmacy of East China University of Science and Technology for graphical picture preparation.

References and notes

1. Ogiso, H.; Ishitani, R.; Nureki, O.; Fukai, S.; Yamanaka, M.; Kim, J.-H.; Saito, K.; Sakamoto, A.; Inoue, M.; Shirouzu, M.; Yokoyama, S. *Cell* **2002**, *110*, 775.
2. Bishayee, S. *Biochem. Pharmacol.* **2000**, *60*, 1217.
3. Holbro, T.; Civenni, G.; Hynes, N. E. *Exp. Cell Res.* **2003**, *284*, 99.
4. Hynes, N.; Horsch, K.; Olayioye, M.; Badache, A. *Endoc. Relat. Cancer* **2001**, *8*, 151.
5. Smaill, J. B.; Palmer, B. D.; Rewcastle, G. W.; Denny, W. A.; McNamara, D. J.; Dobrusin, E. M.; Bridges, A. J.; Zhou, H.; Showalter, H. D. H.; Winters, R. T.; Leopold, W. R.; Fry, D. W.; Nelson, J. M.; Slintak, V.; Elliot, W. L.; Roberts, B. J.; Vincent, P. W.; Patmore, S. J. *J. Med. Chem.* **1999**, *42*, 1803.
6. Tsou, H.-R.; Mamuya, N.; Johnson, B. D.; Reich, M. F.; Gruber, B. C.; Ye, F.; Nilakantan, R.; Shen, R.; Discafani, C.; DeBlanc, R.; Davis, R.; Koehn, F. E.; Greenberger, L. M.; Wang, Y.-F.; Wissner, A. *J. Med. Chem.* **2001**, *44*, 2719.
7. Wissner, A.; Berger, D. M.; Boschelli, D. H.; Floyd, M. B.; Greenberger, L. M.; Gruber, B. C.; Johnson, B. D.; Mamuya, N.; Nilakantan, R.; Reich, M. F.; Shen, R.; Tsou, H.-R.; Upeslacis, E.; Wang, Y. F.; Wu, B.; Ye, F.; Zhang, N. *J. Med. Chem.* **2000**, *43*, 3244.
8. Ducray, R.; Ballard, P.; Barlaam, B. C.; Hickinson, M. D.; Kettle, J. G.; Ogilvie, D. J.; Trigwell, C. B. *Bioorg. Med. Chem. Lett.* **2008**, *18*, 959.
9. Mastalerz, H.; Chang, M.; Chen, P.; Fink, B. E.; Gavai, A.; Han, W.-C.; Johnson, W.; Langley, D.; Lee, F. Y.; Leavitt, K.; Marathe, P.; Norris, D.; Oppenheimer, S.; Sleczka, B.; Tarrant, J.; Tokarski, J. S.; Vite, G. D.; Vyas, D. M.; Wong, H.; Wong, T. W.; Zhang, H.; Zhang, G. *Bioorg. Med. Chem. Lett.* **2007**, *17*, 4947.
10. Mastalerz, H.; Chang, M.; Gavai, A.; Johnson, W.; Langley, D.; Lee, F. Y.; Marathe, P.; Mathur, A.; Oppenheimer, S.; Tarrant, J.; Tokarski, J. S.; Vite, G. D.; Vyas, D. M.; Wong, H.; Wong, T. W.; Zhang, H.; Zhang, G. *Bioorg. Med. Chem. Lett.* **2007**, *17*, 2828.
11. Xu, G.; Abad, M. C.; Connolly, P. J.; Neeper, M. P.; Struble, G. T.; Springer, B. A.; Emanuel, S. L.; Pandey, N.; Gruninger, R. H.; Adams, M.; Moreno-Mazza, S.; Fuentes-Pesquera, A. R.; Middleton, S. A. *Bioorg. Med. Chem. Lett.* **2008**, *18*, 4615.
12. Xu, G.; Searle, L. L.; Hughes, T. V.; Beck, A. K.; Connolly, P. J.; Abad, M. C.; Neeper, M. P.; Struble, G. T.; Springer, B. A.; Emanuel, S. L.; Gruninger, R. H.;

Pandey, N.; Adams, M.; Moreno-Mazza, S.; Fuentes-Pesquera, A. R.; Middleton, S. A.; Greenberger, L. M. *Bioorg. Med. Chem. Lett.* **2008**, *18*, 3495.
13. Rusnak, D. W.; Lackey, K.; Affleck, K.; Wood, E. R.; Alligood, K. J.; Rhodes, N.; Keith, B. R.; Murray, D. M.; Knight, W. B.; Mullin, R. J.; Gilmer, T. M. *Mol. Cancer Ther.* **2001**, *1*, 85.
14. Wood, E. R.; Truesdale, A. T.; McDonald, O. B.; Yuan, D.; Hassell, A.; Dickerson, S. H.; Ellis, B.; Pennisi, C.; Horne, E.; Lackey, K.; Alligood, K. J.; Rusnak, D. W.; Gilmer, T. M.; Shewchuk, L. *Cancer Res.* **2004**, *64*, 6652.
15. Rewcastle, G. W.; Denny, W. A.; Bridges, A. J.; Zhou, H.; Cody, D. R.; McMichael, A.; Fry, D. W. *J. Med. Chem.* **1995**, *38*, 3482.
16. Bridges, A. J.; Zhou, H.; Cody, D. R.; Rewcastle, G. W.; McMichael, A.; Showalter, H. D. H.; Fry, D. W.; Kraker, A. J.; Denny, W. A. *J. Med. Chem.* **1996**, *39*, 267.
17. Barker, A. J.; Gibson, K. H.; Grundy, W.; Godfrey, A. A.; Barlow, J. J.; Healy, M. P.; Woodburn, J. R.; Ashton, S. E.; Curry, B. J.; Scarlett, L.; Henthorn, L.; Richards, L. *Bioorg. Med. Chem. Lett.* **2001**, *11*, 1911.
18. Smaill, J. B.; Showalter, H. D. H.; Zhou, H.; Bridges, A. J.; McNamara, D. J.; Fry, D. W.; Nelson, J. M.; Sherwood, V.; Vincent, P. W.; Roberts, B. J.; Elliott, W. L.; Denny, W. A. *J. Med. Chem.* **2001**, *44*, 429.
19. Pawar, V. G.; Sos, M. L.; Rode, H. B.; Rabiller, M.; Heynck, S.; van Otterlo, W. A. L.; Thomas, R. K.; Rauh, D. *J. Med. Chem.* **2010**, *53*, 2892.
20. Mosmann, T. J. *Immunol. Methods* **1983**, *65*, 55.
21. Mahboobi, S.; Sellmer, A.; Winkler, M.; Eichhorn, E.; Pongratz, H.; Ciossek, T.; Baer, T.; Maier, T.; Beckers, T. *J. Med. Chem.* **2010**, *53*, 8546.
22. Maestro, Schrödinger, *LLC*; New York: NY., 2008.
23. Ligprep, Schrödinger, *LLC*; New York: NY, 2008.